06EX1278

2006 IEEE International Vacuum Electronics Conference

held jointly with

2006 IEEE International Vacuum Electron Sources

IEEE

IVEC/IVESC 2006

（下册）

April 25 - 27, 2006

Portola Plaza Hotel
Monterey, California, USA

Sponsored by the
IEEE Electron Devices Society

http://ivec2006.org

The Simplest Ubitron in Crossed Fields

M. Fuks and E. Schamiloglu

Department of Electrical & Computer Engineering, University of New Mexico
MSC01 1100, 1 University of New Mexico, Albuquerque NM 87131-0001 USA
E-mail: edl@ece.unm.edu Phone: (505) 277-4423 Fax: (505) 277-1439

We present the simplest type of an M-type ubitron in the form of a magnetically insulated coaxial diode with a cathode consisting of N individual longitudinal strips (explosive electron emitters) periodically arranged on an imaginary cylindrical surface (Fig. 1) mounted coaxially within a pipe. The configuration of the cross-section of the cathode strips is arbitrary. This cathode, the so-called "transparent cathode" [1] serves several functions:

1. Individual strips are sources of electrons forming a solid electron sheath that moves around the cathode in crossed fields, the applied uniform axial magnetic field B_{0z} and transverse electric field E_0 of the applied voltage U. In regions outside the cathode the electric field is radial, E_{0r}, which promotes the azimuthal drift of electrons.
2. The cathode strips also form a wiggler, producing azimuthally modulated transverse magnetic fields owing to the axial currents along the strips. Thus, the electron sheath drifts around the cathode through a transverse periodic magnetic field, similar to the rippled-field magnetron (RFM) [2]. However, unlike the complicated system in a RFM that utilized periodic permanent magnets (Fig. 2), the suggested design is much simpler. In addition, the cathode radius can be selected to provide a suitable electron current, unlike the large unwanted axial electron current in the RFM. (The RFM has a narrow gap between electrodes, which is necessary to provide a detectable radial magnetic field; otherwise the magnetic field will basically be concentrated between adjacent magnets). Examples of the azimuthal distributions of the periodic radial magnetic field and leakage current are shown in Figs. 3 and 4.
3. As discussed in [1], for wave electric fields without an axial component (TE modes), such a cathode is transparent. Therefore, these wave fields are strong in the region of the electron flow, which improves the interaction between the fields and electrons, unlike the case for a solid cathode, where the tangential fields go to zero on the cathode surface.
4. The cathode comprises a periodic electrodynamic system that gives rise to azimuthal spatial harmonics of the eigenmodes of the ubitron that can lead to additional resonant interactions.

In spite of the simple design the operation of this device is not easily predicted, although we can definitely state that in the ubitron, as in the RPM, azimuthal recurrence provides inner feedback that leads to an absolute instability in the electron sheath–electromagnetic field interacting system; in other words, the ubitron can operate as an oscillator.

Computer simulations of some examples using the 3-D particle-in-cell code MAGIC demonstrate the presence of very sensitive resonant dependencies of power and spectrum of radiation to variations in the applied voltage U and magnetic field B_{0z} at time of observation of about 100 ns. For parameters of planned experiments using a 600 keV electron accelerator (an ubitron with anode radius $R_a = 2.5$ cm, cathode radius $R_c = 0.9$ cm, and the radius of each of the $N = 6$ rods is $r_0 = 0.1$ cm) we found that the calculated radiation power about $P \approx (160 - 190)$ MW at frequency $f = 4$ GHz with efficiency up to 14% was achieved in 20 ns in the narrow interval of magnetic fields $\Delta B/B \approx 0.01$ in the region of $B_{0z} = 1.05$T when the voltage risetime $t_U = 1$ ns (Fig.5). Outside this interval the radiation power decreases more than 10 times. The suggested oscillator can be interesting owing to its simple design and simple control of characteristics of radiation (with single frequency radiation as well as multi-mode one) by variation of the value and direction of the guide magnetic field.

[1] M. Fuks and E. Schamiloglu, Phys. Rev. Lett., vol. 95, pp. 205101-4, 2005.

[2] G. Bekefi, Appl. Phys. Lett., vol. 40, pp. 578-580, 1982.

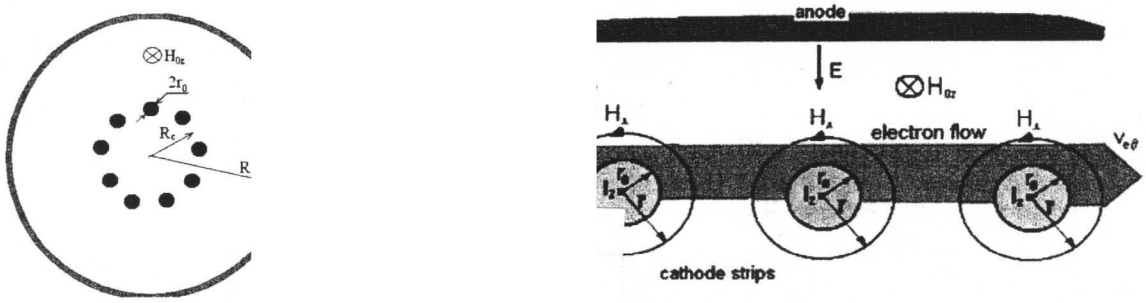

Fig.1. Left: ubitron as a magnetically insulated diode with longitudinal cathode strips arranged on cylindrical surface, coaxially mounted within a pipe; right: fields in the ubitron.

1-4244-0108-9/06/$20.00 © 2006 IEEE

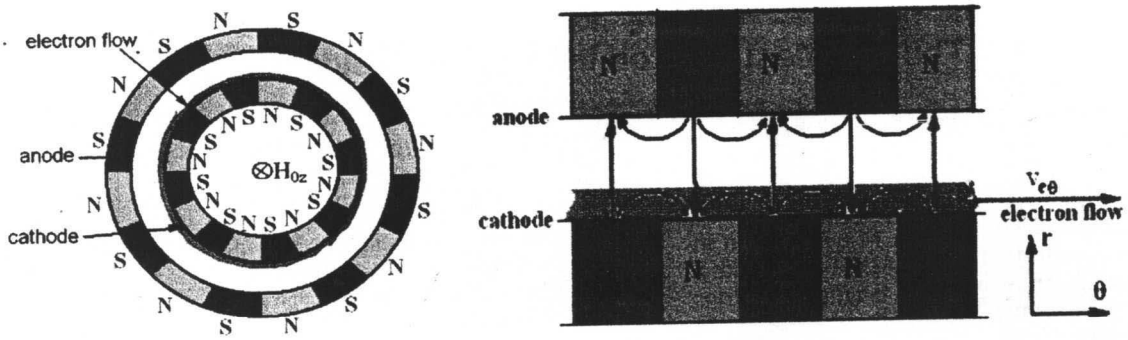

Fig.2. Left: a rippled field magnetron; right: configuration of the periodic magnetic field in the RFM.

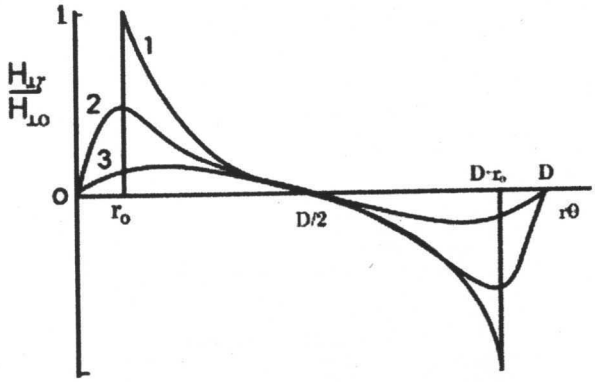

Fig.3. Azimuthal distributions of radial magnetic field $H_{\perp r}$ over the cathode period D for a radius $R = R_c$ (1), $R = R_c + r_0$ (2) and $R = R_c + 2r_0$ (3). ($H_{0\perp}$ is the magnetic field on strip surface).

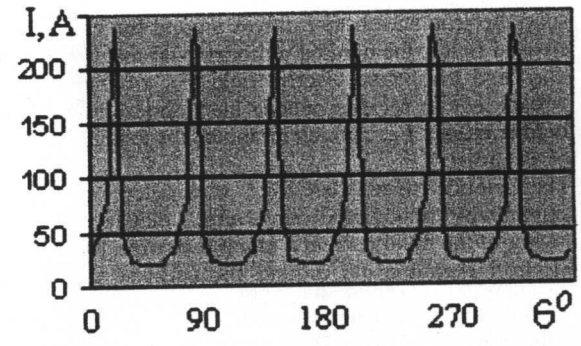

Fig.4. Azimuthal distribution of leakage current at the time 40ns.

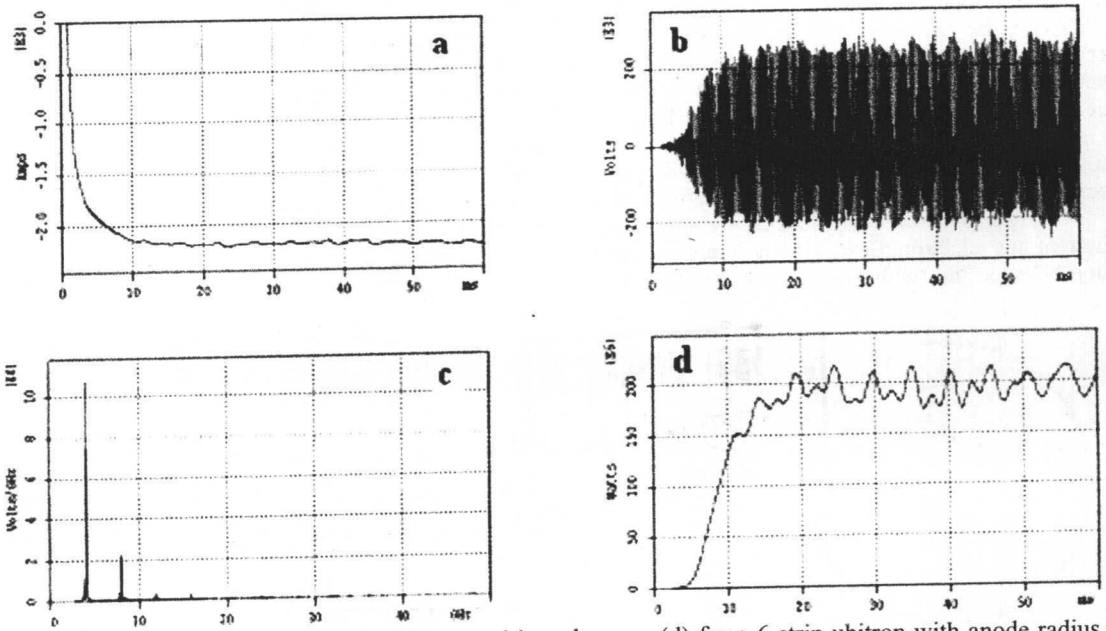

Fig.5. Axial current (a), radiation field (b), spectrum (c), and power (d) for a 6-strip ubitron with anode radius 2.5 cm and cathode radius 0.9 cm when the applied voltage $U = 0.6$ MV with risetime $t_U = 1$ ns and axial magnetic field $B_{0z} = 1.045$ T.

Robust Design Algorithm for High-Frequency Traveling-Wave Tube Slow-Wave Circuits

Jeffrey D. Wilson
NASA Glenn Research Center
21000 Brookpark Rd., MS 54-5, Cleveland, OH, USA, 44135 (Jeffrey.D.Wilson@nasa.gov)

Christine T. Chevalier
Analex Corporation
21000 Brookpark Rd., MS GES-AOS, Cleveland, OH, USA, 44135

Abstract: *An optimization algorithm has been developed to provide robust designs for slow-wave circuits of high frequency traveling-wave tubes. A simulated statistical performance test of a robust design for a 94-GHz folded waveguide circuit shows significantly less sensitivity to dimensional tolerance variations.*

Keywords: traveling-wave tube; optimization; simulated annealing; robust design; algorithm.

Introduction

In the frequency regime of 60-600 GHz, vacuum electronics amplifiers have tremendous potential for high data rate secure communications, surveillance, and remote sensing. However dimensional variations resulting from conventional micromachining techniques that are adequate for lower frequency operation can be relatively large enough to cause serious degradation and variation of performance at higher frequencies. When this is the case, conventional design optimization procedures provide non-robust designs and the actual amplifier performance can substantially under-perform the predicted design performance. Thus, a new optimization procedure was developed to provide robust designs for high performance millimeter-wave and terahertz communications amplifiers.

Analysis

The effects of dimensional variations on the phase shift, interaction impedance, and attenuation of several traveling-wave tube (TWT) slow-wave circuits were investigated at a frequency of 94 GHz with the 3-D electromagnetic simulation software CST Microwave Studio (MWS) [1]. This sensitivity analysis determined that the folded waveguide (Figure 1) was the most robust circuit.

MWS was then used to design the folded waveguide geometry for optimal power gain and to determine the dependence of the phase shift, interaction impedance, and attenuation on the period length 'p'. This information is used for input into the NASA Coupled-Cavity TWT Code [2] which calculates the interaction between an electron beam and the RF wave traveling through an entire slow-wave circuit consisting of several hundred periods of folded waveguide.

After the cold-test information is input into the NASA TWT Code, optimization routines in the code determine the lengths of the periods in the circuit that produce the best RF efficiency performance. Previously algorithms based on simulated annealing have been developed to optimize RF efficiency at a single frequency [3] and over a frequency bandwidth [4]. In this project, we created and developed an algorithm based on simulated annealing to optimize RF efficiency while taking into account dimensional tolerances. The details of the new algorithm will be presented at the conference.

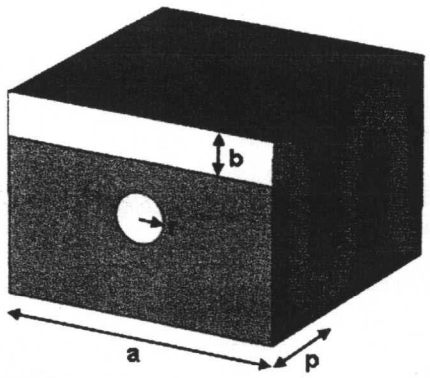

Figure 1. Folded-waveguide circuit geometry.

Results

Two 94-GHz folded waveguide traveling-wave tube slow-wave circuits were designed, each with an input section, sever, and output section. The phase velocity taper in the first circuit was designed with the standard simulated annealing optimization algorithm [3]; the taper for the second circuit was designed with the new robust optimization algorithm.

In order to compare the designs, we performed Monte Carlo (MC) simulations consisting of 200 runs each on the standard and robust circuit designs. In practice, the lengths are generally either longer or shorter than the nominal values. Thus in the first MC simulation set, we assumed that the lengths had a pseudo Gaussian distribution centered at the nominal values plus half of the tolerance value. For each of the 200 MC runs, each individual cavity length of the slow-wave circuit is randomly assigned a value with

1-4244-0108-9/06/$20.00 © 2006 IEEE

respect to the nominal value according to this probability distribution. In the second set of MC simulations, the probability distribution was assumed to be a pseudo Gaussian centered at the nominal values minus half of the tolerance value.

For the first set, the results of the MC simulations are very similar for the two designs with average efficiency values of 4.92% for the robust design and 5.12% for the standard design. However for the second set, the MC results which are shown in Figure 2 are dramatically different for the two designs. While the average efficiency value with the standard design is only 1.31%, it is 4.09% with the robust design. This represents an increase by a factor of 3.12. Thus the effect of the robust design is to broaden the 'sweet spot' around the nominal design values. Since we don't know a priori whether manufactured circuits will have period lengths either shorter or longer than the specified nominal lengths, the robust design is more likely to produce favorable performance.

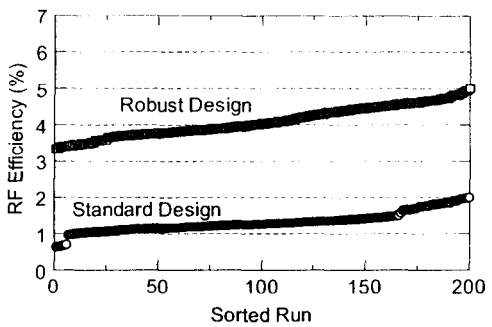

Figure 2. Distributions of RF efficiencies of robust and standard designs with Monte Carlo simulations for period lengths with average values shorter than nominal values.

Conclusions

In this project, we have created and developed a design optimization algorithm for improving the RF power, RF efficiency, and robustness of high frequency vacuum electronic amplifiers while taking into account the sensitivity to dimensional variations. The algorithm was tested by using it to design a 94-GHz folded waveguide circuit. The simulated statistical performance of this design with regard to pseudorandom dimensional variations was determined and compared to that of a design optimized with a standard method. The results showed that the robust design is comparable to the standard design when the circuit period lengths are on average longer than the nominal values. However when the circuit period lengths are shorter, the robust design is far superior. This indicates that the robust optimization algorithm produces a design that is significantly less sensitive to dimensional tolerance variations. At higher frequencies with corresponding higher relative tolerances, we expect that the superiority of robust design performance will be even more significant.

References

1. http://www.cst.de.
2. Wilson, J. D., "Revised NASA Axially Symmetric Ring Model for Coupled-Cavity Traveling-Wave Tubes," NASA Technical Paper 2675, Jan. 1987.
3. Wilson, J. D., "A Simulated Annealing Algorithm for Optimizing RF Power Efficiency in Coupled-Cavity Traveling-Wave Tubes," *IEEE Trans. Electron Devices*, Vol. 44, no. 12, pp. 2295-2299, Dec. 1997.
4. Wilson, J. D., "Design of High-Efficiency Wide-Bandwidth Coupled-Cavity Traveling-Wave Tube Phase Velocity Tapers with Simulated Annealing Algorithms," *IEEE Trans. Electron Devices*, Vol. 48, no. 1, pp. 95-100, Jan. 2001.

The Determination of Tape Helix Cold Test Parameters Using Fourier and Convolution Techniques

Vinh Cun
Communications & Power Industries (CPI)
607 Hansen Way, Bdlg 1
Palo Alto, CA 94304
Phone (650) 846-2905
Email: vinh.cun@cpii.com

Abstract: *A program was written to predict cold test parameters of helix traveling wave tubes. Parameters such as dispersion, interaction impedance, and phase velocity can be obtained in that the flexibility of the program allows for quick simulations compared to commercial CAD packages.*

Keywords: traveling wave tube; cold test; tape helix; interaction impedance, dispersion

Introduction

Historically, helix cold test simulations have not been able to accurately predict parameters well enough to build a device within specifications the first time. A computer program was created to determine the cold test parameters of helix traveling wave tubes. The implementation is based on techniques described in [1], where the helix structure and surrounding support rods are transformed to Fourier space. The transformed structure is then convoluted with the field harmonics to calculate cold test parameters such as omega-beta diagram, phase velocity, and interaction impedance. This technique was chosen since the theory in [1] yielded an exact solution. The speed and flexibility of the program allows for changing of parameters without the time-consuming process of redrawing the structure and resimulation as done in commercial CAD packages. Convergence is controlled by the number of harmonics desired in the calculation. Below are representations of a tape helix with N = 5, 10, 25 harmonics, and as the number of harmonics increase, the representation develops into a tape helix. The computer program is written in MathCad for its programmability and mathematics library. Experimental data will also be compared to the program to verify its results.

Representation of helix structure at OD using 5 harmonics

Figure 1. Helix representation using 5 harmonics

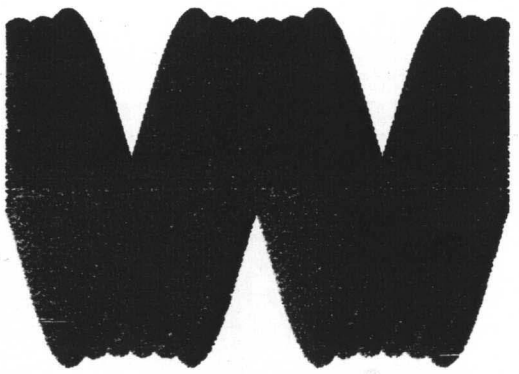

Representation of helix structure at OD using 10 harmonics

Figure 2. Helix representation using 10 harmonics

1-4244-0108-9/06/$20.00 © 2006 IEEE

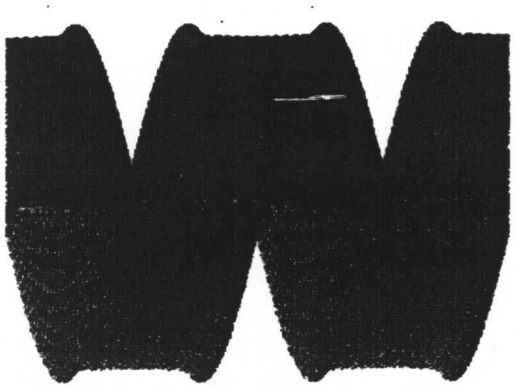

Representation of helix structure at OD using 25 harmonics

Figure 3. Helix representation using 25 harmonics

References

[1] T. Wessel-Berg, "CAD of Tape Helix Circuits for Traveling Wave Tubes by Convolution Methods," *IEEE Trans. Electron Devices*, vol. 51, no. 11, pp 1918-1927, Nov. 2004

The Field Marshal Electromagnetic Simulation Environment[1]

R. H. Jackson, M. McLay and R. P. Joshi[†]

Calabazas Creek Research, Inc., Saratoga, CA
[†]Old Dominion University, Norfolk, VA
1331 Annapolis Way
Grayson, GA 30017
(404) 518-0200 Tel
(678) 623-0128 Fax
rhj@CalCreek.com

The Field Marshal (FM) simulation environment is aimed at small research groups involved in electromagnetics design and analysis. Project goals include consistent user interface, single-geometry/multiple-tools and inclusion of legacy codes. A key objective is usability, maintainability, and extensibility by researchers who are not expert programmers. Four primary elements are necessary to cost-effectively achieve this: finite difference techniques, multigrid techniques, a modern scripting environment (e.g. Python), and internet-based distributed development.

Architecture

The design process is viewed from the standpoint of single researcher or small group R&D projects. This implies a need for multiple design tools (many of which could be legacy codes) applied to different aspects of and/or regions of a single "device," which may be simple or a complex amalgam of elements. For this approach to be effective, the multiple design tools must be driven by a single geometry. In addition, a common user interface for the various tools is *highly* desirable. These considerations have to be coupled with the need, inherent in R&D, for flexibility and extensibility of tools without requiring the user to become an expert programmer. Field Marshal addresses these issues in the following way. The simulation process is broken roughly into domains that group typical user activities in the simulation process and provide logical transition points for connection to legacy tools. Within each of these domains, there are "components" that implement Field Marshal methods. This abstraction permits FM to provide a reasonably consistent interface to the user across a wide range of simulation tools. Field Marshal domains include the following:

- Parameter Entry
- Geometry Entry
- Parameter-Geometry Connection
- Parameter and Geometry Translation
- Simulation
- Data Management
- Graphics and Visualization

Third-party CAD software, while attractive at first glance, has many problems when looked at in detail. For the majority of simulation needs, commercial CAD systems are overkill. Among other problems, they lack the simplicity and flexibility that researchers need to rapidly explore new ideas. The Field Marshal SimpleCAD component provides a simple 2D geometric capability that is tightly focused on simulation.

Finite Differences for Non-Conformal Boundaries

Shown below is a Taylor expansion polynomial that inherently satisfies Laplace's equation in a homogeneous region around a point.

$$U(\xi,\eta) = U_p + a_{10}\xi + a_{11}\eta + a_{20}(\xi^2 - \eta^2) + a_{21}\xi\eta + a_{30}\xi(\xi^2 - 3\eta^2) + a_{33}\eta(\eta^2 - 3\xi^2) + \cdots$$

A matrix equation relating the polynomial and potential values at grid points can be written. This relation can be used to estimate the central-point potential by multiplying the potential vector, **U**, by a *weight* vector $\mathbf{v}^T$ (the finite-difference coefficients). The goal is to determine **v** such that a high order estimate is obtained. This usually involves determining the *null-space* of a matrix constructed from the offsets of the stencil points relative to the central point. A new algorithm will be presented which only requires a standard matrix inversion to determine the finite-difference coefficients.

Multigrid: A Simple Example

Multigrid is a set of techniques employing nested grids and grid patches to increase solution speed and provide variable resolution. As an example, a thin-plate, parallel plate capacitor was solved two ways: a single grid and three nested grids with the final grid at single-grid resolution. The single grid calculation required 559 iterations to converge. The nested-grid required a total of 635 iterations, but only 371 were at the single grid resolution. The other 264 iterations were at lower grid resolutions and required significantly less time. The level-1 and level-3 solutions are shown below.

[1]Work supported by the Air Force Office of Scientific Research under SBIR contract FA9550-04-C-0080.

1-4244-0108-9/06/$20.00 © 2006 IEEE

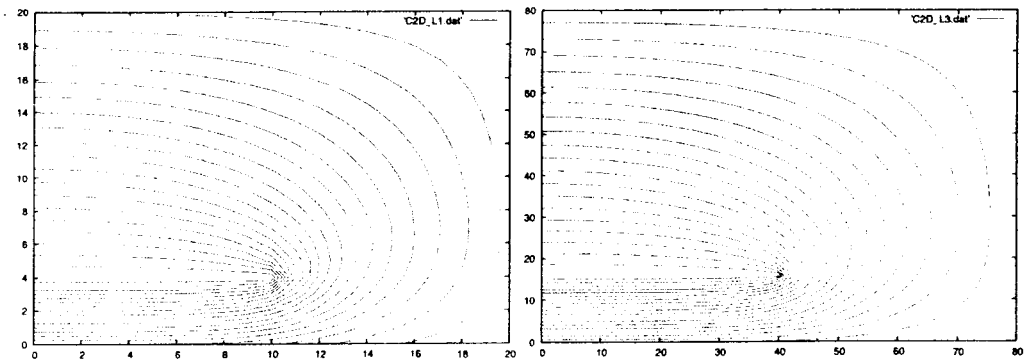

Summary

The Field Marshal project is aimed at providing a consistent user interface and single-geometry view to multiple design tools for researches who are non-expert programmers. Details of the Field Marshal environment and components will be presented. Information and current status of the project can be found at www.FieldMarshal.org.

Analysis with Code Dev. 5.0 of Output Characteristics of Coupled Cavity TWT with Below-Cutoff Sections and with Direct and Inverse Bands Sequence

A. V. Konnov, A. V. Malykhin, V. V. Petenkova

FSUE "R & P Corp. "Toriy", Obrucheva str., 52,
117393 Moscow, Russia,
E-mail: npptoriy@mtu-net.ru,
Tel./Fax: +7 495 331 34 22

G. V. Ruvinskiy, T. I. Chernobay, D. S. Scherbakov

FSUE "R & P Corp. "Istok", 2-ya Vokzal'naya str.,
Fryazino-141190, Moscow region, Russia,
E-mail: istok@elnet.msk.ru,
Tel./Fax: +7 495 745 15 57

Earlier [1] code Dev.5.0 has been developed. This code is intended for computation of the performances of coupled cavity TWTs (CCTWT) and hybrid O-type devices. This code is based on the model of circuit cavity as lumped elements scheme of the common kind [2]. The ability of adequately simulate the output frequency characteristics of multiple-section CCTWT with the shifted band of intermediate section beyond the working frequency band is the most important test of code. In this report the results of simulation the performances of three-sectional K_u-band CCTWT and three-sectional X-band interdigital structure TWT (ISTWT) (both TWTs are produced by FSUE "Istok") are presented. The frequencies of π-mode cutoffs of the second sections are shifted up beyond the working bands. Particular feature of test is that the lower band is "cavity" band and the upper band is 'slot" band in CCTWT (Fig. 1a) but in ISTWT the lower band is 'slot" band and the upper band is "cavity" band (Fig. 1b). In the other words ISTWT has inverse bands sequence.

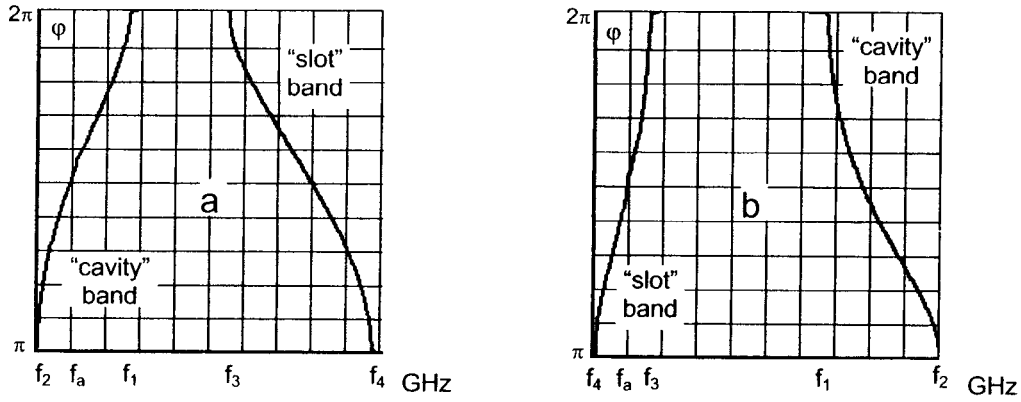

Figure 1. Dispersion curves of regular parts of the 1-st and the 3-d section of K_u-band CCTWT (a) and X-band ISTWT (b)

The set of initial data [2] related to the regular parts of sections is represented in the table below.

	CCTWT			ISTWT		
Data	**Section 1**	**Section 2**	**Section 3**	**Section 1**	**Section 2**	**Section 3**
f_1, GHz	21.4030	23.3109	21.4030	19.7630	22.9010	19.7630
f_a, GHz	18.1221	19.3221	18.1221	9.3821	10.1700	9.3821
f_2, GHz	16.2500	17.1250	16.2500	26.5860	26.6200	26.5860
f_3, GHz	27.0486	26.8280	27.0486	10.5340	11.2330	10.5340
f_4, GHz	35.3810	36.3960	35.3810	7.7140	8.4200	7.7140
ρ, Ohm	76.0000	86.5000	76.0000	71.2000	80.0000	71.2000
Q_o	600.0	600.0	600.0	1000.0	1000.0	1000.0
$Zs(f_a)/Zg(f_a)$	0.3000	0.3000	0.3000	0.2490	0.3000	0.2140

1-4244-0108-9/06/$20.00 © 2006 IEEE

Here the frequencies f_1-и f_2 are the frequencies of 2π- and π-modes of the "cavity" band, f_3 and f_4 are the frequencies of 2π- and π- modes of the "slot" band. The frequency f_a is the frequency of $3/2\pi$-mode of the "cavity" band in CCTWT but the frequency of $3/2\pi$-mode of the "slot" band in ISTWT.

The R/Q_0 ratio (ρ) and quality Q_0 of cavity are defined at the frequency of 2π-mode f_1 in the "cavity" band for both TWTs.

Normalized wave (slot) impedance of the circuit $Zs(f_a)/Zg(f_a)<1$, where $Zg(f_a)$ is interaction (gap) impedance at the frequency f_a. The ratio $Zs(f_a)/Zg(f_a)$ may be defined arbitrarily (within the range of physical existence of the scheme elements) because this value is used only by matching. The similar set of parameters of matching and terminal cavities is used for tuning of matching curves of TWT sections (Fig.2 a,b).

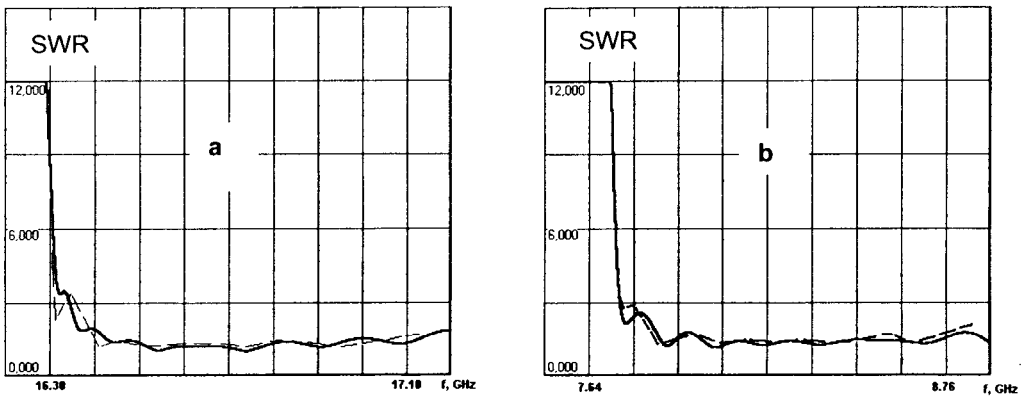

Figure 2. The output SWR curves of 3-d sections. **a** – CCTWT, **b** – ISTWT. Dashed lines – measured SWR.

Amplitude-frequency curves of K_u-band CCTWT (beam voltage 29.0. kV, current 2.08 A), simulated and measured near saturation regime are presented in Fig 3a. Driven power is 10 mW. Amplitude-frequency curves of X-band ISTWT (beam voltage 10.8. kV, current 0.89 A) simulated and measured in saturation regime are presented in Fig 3b. Driven power is 0.3 W. In both devices a satisfactory agreement between simulation and experiment are observed.

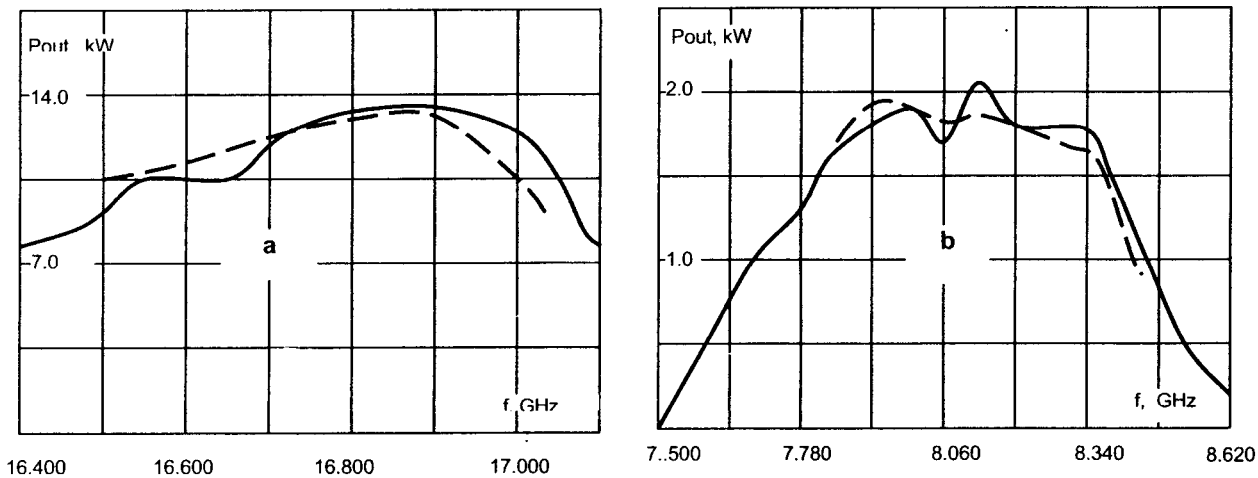

Figure 3. Amplitude-frequency curves: **a**- CCTWT, **b** – ISTWT. Dashed lines – experimental curves.

References

1. Konnov A.V., Malykhin A.V., "Frequency-domain code Dev.5.0 for analysis of coupled–cavity traveling wave tubes, klystrons and their hybrids", *Proceedings of VI* ***IVEC 2005*** *conference*, Noordwijk, Netherlands, pp.195-198.
2. Malykhin A.V., Konnov A.V., Komarov D.A. "Synthesis of six-pole network simulating of coupled cavity chain characteristics in two passbands", *Proceedings of IV* ***IVEC 2003*** *conference*, Seoul, Korea, pp.159-160.

Recent Developments to TWTCAD Integrated Framework

Li Bin, Yang ZhongHai, Li JianQing, Zhu XiaoFang, Huang Tao, Hu Quan, Liao Li, Xiao Li, Gao Peng, Zeng BaoQing, Yao LieMing, He GuoXian

School of Physical Electronics, University of Electronic Science and Technology of China
NO.4, Section 2, North Jianshe Road, Chengdu, P. R. China 610054
Email: libin@uestc.edu.cn, Tel: 86-28-8320-3371, Fax: 86-28-8320-3371

Abstract: *Recent developments to TWT Integrated Framework, a 2D modeling and simulation code suite for traveling wave tube, will be presented. Two codes, UESTC_PPM and UESTC_DB, are added to TWTCAD. Existed another four codes are improved. TWTCAD is applying and validating in microwave industry.*

Keywords: Traveling-Wave Tubes (TWTs); modeling and simulation.

1. Introduction

TWTCAD Integrated Framework is a 2D modeling and simulation code suite for traveling wave tube, which includes six codes and all these codes, can be invoked in one dialoged code. The six codes are UESTC_Gun, UESTC_PPM, UESTC_HelixCT, UESTC_BWI, UESTC_MDC, and UESTC_DB. All these codes are written by C++ language in Microsoft Windows platform.

2. Code List

UESTC_Gun

UESTC_Gun, A 2D gun code, in its model, space charge effect, initial thermal velocity of cathode, self-magnetic field effect of beam, effect of shadow grid/control grid to beam, and effect of magnetic field in transition region are taken into account.

UESTC_PPM

Period permanent magnet focus system is simulated by UESTC_PPM. Like UESTC_Gun, finite difference method is used. Mesh is generated automatically. Magnetic field curve on axial is calculated. Distribution of magnetic field on axial and radial are simulated.

UESTC_HelixCT

In UESTC_HelixCT, a 2D helix circuit code test code, sheath model and tape model are applied. Some used helix circuits are modeled. The dispersion and impedance, resulting from UESTC_HelixCT, will be input parameter for UESTC_BWI.

UESTC_BWI

UESTC_BWI, 2D large signal code, is based on Rowe model and Vainstein model including harmonics. 2D model represents the beam as a series of rings that may expand radially, as well as move axially. When the rings approach each other from infinity, the forces exerting between them remain constant, being independent of distance, and electron overtaking is possible.

UESTC_MDC

The code, named UESTC_MDC, a 2D multistage depressed collector design code, can compute static electric field, injecting electron trajectories, secondary electron trajectories which are produced by injecting electron collision on electrode surface.

UESTC_DB

All input and output parameter from the other five codes is managed by UESTC_DB. Input parameter for the other codes is setting in UESTC_DB and stored in ACCESS database. Output parameter and calculation result from the other codes will be stored in ACCESS database too. All this data can be browed, modify and used to post-process in UESTC_DB.

3. Conclusion

A 2D helix TWT design code suite, is developed, which is used to design helix traveling wave tube with axially symmetry, includes six codes, UESTC_Gun, UESTC_PPM, UESTC_HelixCT, UESTC_BWI, UESTC_MDC and UESTC_DB. It is validating and applying in microwave tube industry.

References

1. T M Antonsen Jr. *et al.* Advances in Modeling and Simulation of Vacuum Electronic Devices. *Proc IEEE*, 1999, 87(5): 804-839.
2. T B Robert *et al.* First pass TWT design success. *IEEE Trans on Electron Devices*, 2001, 48(1): 176- 178.
3. C L Chang et al. Application and validation of the helix TWT design code suite. IVEC 2002. April 2002: 13-14.
4. Li Bin. Study of Gain and Phase Matched Characteristic of Traveling Wave Tube. Ph. D. Thesis, Univ of Elec Sci & Tech of China (2003)
5. Li J Q. TWT Three-Dimensional Nonlinear Theory and its Network Parallel Computing. Ph. D. Thesis, Univ of Elec Sci & Tech of China (2003)

1-4244-0108-9/06/$20.00 © 2006 IEEE

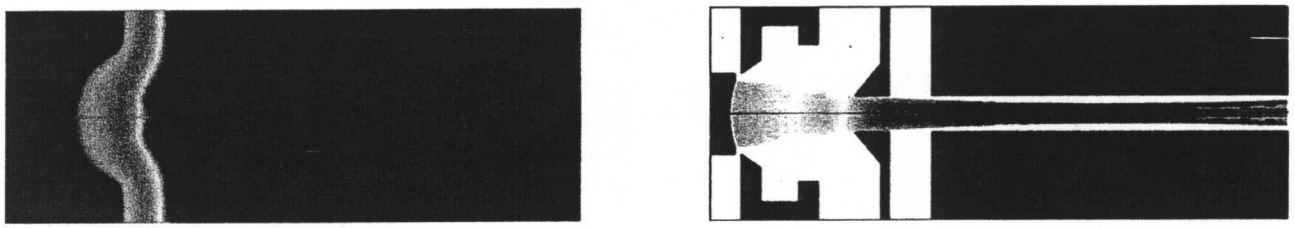

Figure 1. Electron gun simulation, electrical potential (left) and trajectory (right)

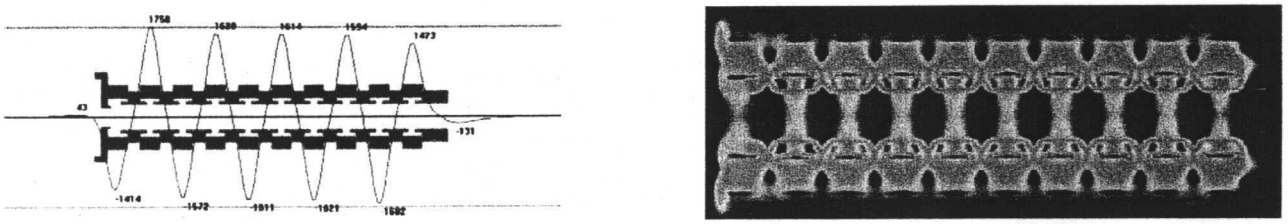

Figure 2. PPM simulation, B_z

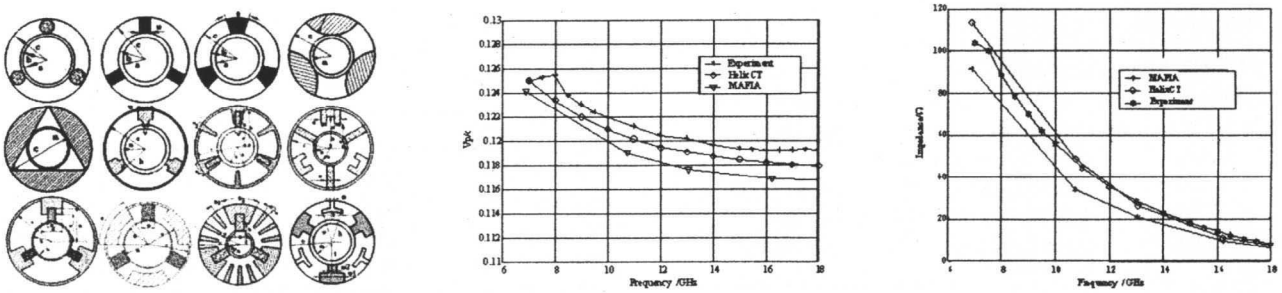

Figure 3. Helix circuit simulation, used circuit (left), dispersion (mid) and impedance (right)

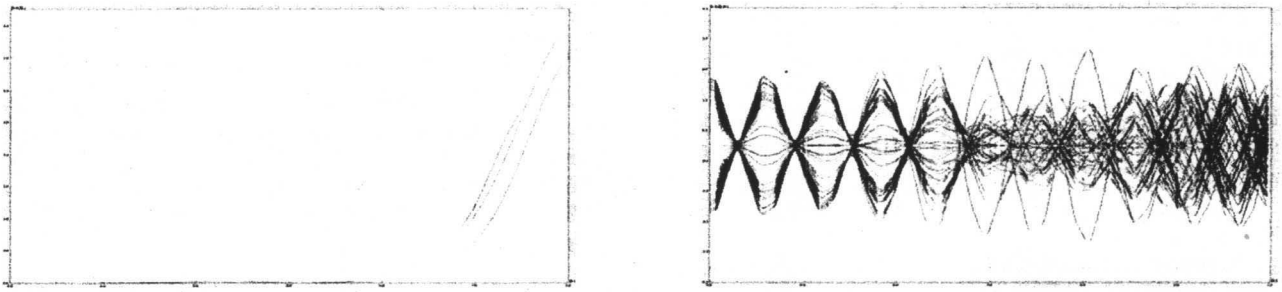

Figure 4. Beam and wave interaction simulation, output power (left) and electron trajectory (right)

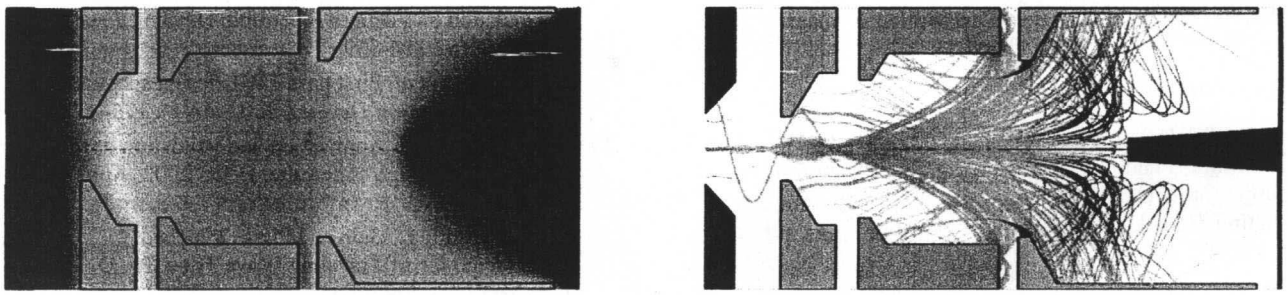

Figure 5. A 4 stage MDC simulation, electrical potential (left) and trajectory include second electron (right)

Electron Beam Transverse Waves and Microwave Electronics

Vladimir A. Vanke
M.V. Lomonosov Moscow State University
Moscow 119992, Russia,
Tel: +7 495 132 48 07, E-mail: vanke@orc.ru

Yury A. Budzinskiy, Sergey V. Bykovskiy
SRPC "Istok"
Fryazino Moscow region 141190, Russia,
Tel: + 7 495 465 88 47, E-mail: serbyko@mail.ru

The further development of vacuum microwave electronics encounters fundamental limitations caused by non-linear disgrouping effect of space charge fields in electron beams and needs extraordinary scientific and technical solutions.

In Russia investigations in the new field of microwave electronics based on transverse grouping of homogeneous electron beam (Fig. 1) in circularly polarized electromagnetic fields of slow-wave structures and resonant cavities, were developed rather intensively during last

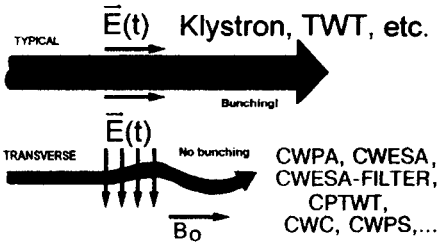

Figure 1. Longitudinal and transverse groupings of the electron beam. E (t) – time-variable electric field, B_o – static magnetic field

several decades [1-7]. The principal advantages of devices based on interaction with slow and fast cyclotron and synchronous waves of the electron beam are:

- The absence of non-linearity connected with formation of space charged bunches. Relativistic (non-linear) dependence of the electron mass on the electron energy is not used here;
- Circular polarization of transverse waves, stability and predictability of their phase velocities make it possible to provide a high level of selectivity in energy exchange with external electromagnetic fields;
- Levels of microwave power in the electron beam can significantly exceed the initial energy of the injected electron beam.

These factors, which seem to be quite simple, allow us to overcome a number of limitations, which restrict today the development of microwave vacuum electronics.

Experimental investigations were tightly combined with computer simulations.

New types of microwave devices with unique set of parameters have been designed, experimentally tested and partly manufactured. The development of these microwave devices became possible because of long-term collaboration of the academic research at Moscow State University and the industrial research and development of the Russian industries.

This report includes the discussion of the physics principles and technology of the following non-traditional devices:

- *CYCLOTRON WAVE PROTECTORS (CWPr, including tunable CWPr)* with super high self-protection against microwave overloads (up to 500-1000 kW in pulse), short restoration time (1-10 ns), absence of leakage power peak, low voltage supply, small size and weight for use as a first element of radar, navigation, and communication receiving systems;
- *LOW-NOISE CYCLOTRON WAVE PARAMETRIC AMPLIFIERS (CWPA, including two-beam CWPA with suppressed idler channel) and CYCLOTRON WAVE ELECTROSTATIC AMPLIFIERS (CWESA)* with low noise temperature (30-150 K), extremely linear phase characteristics, super high self-protection against microwave overloads (up to 500 kW in pulse), short restoration time (1-10 ns), absence of leakage power peak, low voltage supply, small size and weight;
- *NARROW-BAND CONTROLLED CWESA-FILTERS* with low noise temperature (100-200 K), high-speed control of frequency band in wide range (up to 50%), high self-protection, short restoration time (1-10 ns) and absence of leakage power peak;
- *HIGH POWER CIRCULARLY POLARIZED TRAVELLING WAVE TUBES (CPTWT)* with high efficiency (about 35-40% into the load and up to 80% with single-stage depressed collector), wide bandwidth (30% and more) and extremely linear phase-frequency characteristics;
- *HIGH POWER CYCLOTRON WAVE CONVERTERS (CWC, including CWC having decreased magnetic field)* with efficiency of conversion of microwaves into DC - up to 80-90% using single-stage depressed collector, high output power level - up to 50-100 kW, output voltage range - 10-100 kV; having no breakdown and harmonic reradiation problems;
- *KLYSTRONS WITH COMBINED /longitudinal-transverse/ INTERACTION (KCI)* with extended bandwidth (up to 8-10%) and high efficiency (>75-80%) for various power levels (up to 50 kW);

1-4244-0108-9/06/$20.00 © 2006 IEEE

- *CYCLOTRON WAVE PHASE SHIFTERS (CWPS)* for various power levels (from 10 W to 50 kW) with wide phase control range (0-360 grad), low signal losses (< 0.2-0.5 dB), high-speed phase control.

One group of devices is already manufactured commercially (Fig. 2 and Fig. 3, as an example), another group has been under laboratory tests, and finally, there is a great number of interesting and perspective designs based on reliable experimental data.

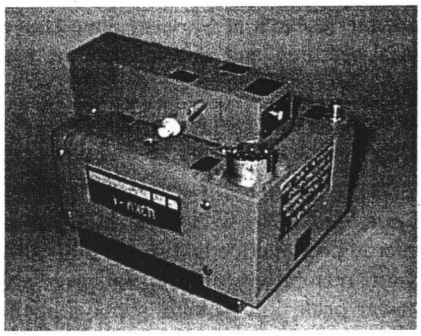

Figure 2. A version of CWPr at 10 GHz (Istok Corp.) in combination with solid-state amplifier

In total more than 10 000 different devices based on electron beam cyclotron waves have been manufactured and sold by the Istok Corp.

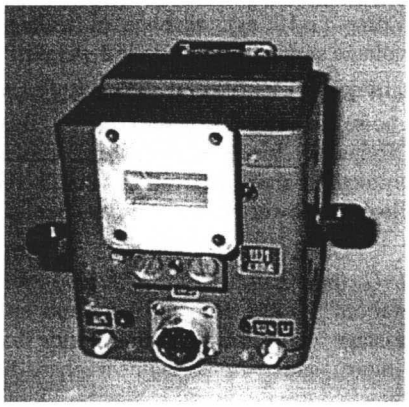

Figure 3. A version of CWESA at 8 GHz (Istok Corp.)

Above listed devices have an essential potential for use in a wide variety of applications including ESR, NMR, MRT, radio astronomy, super high quality military and civil radars, navigation and communication systems as well as the future Space Solar Power for energy supply from Space to the Earth.

An international collaboration could be perspective in this field of vacuum microwave electronics.

It is very likely that there is an opportunity to create some new and improved devices, which are making possible systems having capabilities well beyond any fielded today.

References:

1. Budzinsky Yu.A., Kantyuk S.P., "A New Class of Self-Protecting Low-Noise Microwave Amplifiers". *Proc.IEEE MTT-S Microwave Symposium, Digest, Atlanta,* 1993, No. 2, p. 1123.
2. Vanke V.A., "On Some Microwave Physics Research at Moscow State University and Russian Industries" (Plenary Talk). *1996 IEEE International Conference on Plasma Science (ICOPS'96),* Boston, 1996, June 3-5, p. 62.
3. Vanke V.A., "Microwave Electronics Based on Electron Beam Transverse Waves Using (State-of-the-Art and Perspective. Russian Experience)". *J. of Radioelectronics,* 1999, No.8, http://jre.cplire.ru/jre/aug99/1/text.html
4. Vanke V.A., "Microwave Electronics Based on Electron Beam Transverse Waves Using" (Invited). *Technical Report of the Institute of Electronics, Information and Communication Engineers* (IEICE, Japan), ED99-247, 1999, December 17, p. 1.
5. Boudzinski I.A., Bykovski S.V., "Amplifying and Protective Devices Based on Electron Beam Fast Cyclotron Wave". *The 2nd International Vacuum Electronics Conference,* April 2-4, 2001, Noordwijk, The Netherlands.
6. Boudzinskiy I., Bykovskiy S., Vanke V., "Untraditional Vacuum Microwave Electronics on the Basis of Transverse Waves of an Electron Stream". *Electronics: Science, Technology and Business,* 2005, No. 4, p. 38. (in Russian).
7. Vanke V.A., "Transverse Electron-Beam Waves for Microwave Electronics". *Uspekhi Fizicheskikh Nauk,* 2005, v. 175, No. 9, p. 957, (in Russian). See also: Vanke V.A., "Transverse Electron-Beam Waves for Microwave Electronics". *Physics-Uspekhi,* 2005, v. 48, No. 9, p. 917, (in English).

Comparative Study of Microwave Power Modules (MPM) and Complex Microwave Devices (CMD) Parameters and their Preferable Application Areas

Edward
A.S. Kotov, E.A. Gelvich, A.D. Zakurdayev
FSUE RPC "Istok", 141190, Fryazino, Russia

Mailing address: FSUE RPC "Istok", Vokzalnaya str..2A,141190, Fryazino, Russia
Fax: 7-495-4658686; e-mail: istkor@elnet.msk.ru

The continually increasing number of functions which radio-electronic systems (RES) must provide to meet the current needs for simultaneous radio-location, control, and navigation of multiple objects is leading to an enormous increase of radio-electronic equipment (REE) on board air-, sea- and land-based vehicles. Thus, the mass and volume of a given radio-electronic system – in particular, the transmitter – is a key decisive parameter that determines the acceptability of that system for a given platform. Excessive size and weight are often the principal reasons that render a particular system unacceptable for mobile, on-board applications.

To resolve the competing desires for increased functionality and reduced system size and weight of REE, there were suggested and developed Complex Microwave Devices (CMD) in Russia [1], and Microwave Power Modules (MPM) in USA [2]. Both of them are microwave units that are designed on the principles of integrated low power circuits, and provide the potential to amplify complex signals to the required level. Both of them are constructively- and functionally-integrated devices in which all elements comprising the MPM and CMD are carefully matched to ensure that each constituent element of the device (CMD or MPM) operates in its optimal regime. This functional and constructive integration, supported by the selective matching of the elements comprising the CMD (MPM), and new technologies resulted in a substantial decrease in mass and volume of the devices and of the microwave portion of the REE. Significant increase of the potential abilities of the RES was also achieved.

As a rule, the MPM consists of a solid-state input amplifier which drives a vacuum power booster – a TWT, and a secondary supply unit powering the solid-state and vacuum amplifiers [3]. The structure of CMD is more complicated and depends on the functions which the particular CMD must provide [4]. Low cathode-voltage MBKs are used in CMDs as an output power amplifier. The MPM operate at medium average power ($\leq$ 250 W), CMD operate in a broad range .of output power – from 10-th of watts to 100-th of kW. For comparison of MPM and CMD parameters we consider in this report only the CMD which are near to the MPM in power and destination. Main typical parameters of such miniature multi-functional CMDs are shown in Table 1.

There are developed compact solid-state-vacuum CMDs for on-board applications. These devices are based on solid-state multi-functional signal-creating and driving circuits and high efficient, compact, miniaturized output power MBKs (MMBK). CMD-V is an example of a such .device [5]. Its parameters are near to that shown in Table1, its block diagram and general view are shown below on the last page o the abstract.

CMD-V is able to generate high quality coherent heterodyne and high power signals even in the presence of severe operational conditions: the frequency noise level is less than –90 dBc/Hz at 5 kHz off the carrier frequency, and the carrier instability, $\Delta f/f$, is less than $\pm 10^{-4}$. The most outstanding features are its mass (< 2 kg) and fast turn-on time (< 10 s), producing 300 W of output power. The mechanical design is very robust so as to allow the unit to function in severe mechanical environments for CMD-V. The frequency shift of the output carrier at the intermediate frequency is produced by a phase-locked loop (PLL). This feature enables the design to achieve a low level of parasitic components in the output signal (< –60 dBc). Amplitude modulation of the output signal is implemented by a low voltage current-less electrode. The overall efficiency of CMD-V is $\approx$ 30%. The overall efficiency of the *cm*-band

!44-0108-9/06/$20.00 © 2006 IEEE

MPM is proclaimed in [6] as high as (50-70)%. In accordance with industrial sources this figure is substantially less – about (25-35) % with a 3-4-stage recuperation [7].

The advantage of MPM is its broad amplification band, which is many times more than that of the CMD. But the quality of the signal in this broad band is poor: the power level of the harmonics lies in the interval from -12 dBc up to +1dBc [7]. High quality microwave signal amplification can be achieved in a frequency band which does not exceed 10%. Nevertheless, this value of the high quality amplification band is 2-3 times more than that of the CMD.

One of the main distinctions between the MPM and CMD is the number of functions which can be carried out by the device. The dominant function of the MPM consists in amplification of microwave signals, including complicated ones [3]. The CMD, in addition, is able to create coherent heterodyne and high power signals, provide all types of signal modulation –amplitude, phase, frequency modulation -, frequency shift and multiplication [4]. All these functions are carried out ensuring a high frequency and phase quality of the microwave signal.

On the base of the accomplished analysis there can be made a conclusion that both devices, MPM and CMD, have a good perspective for on-board applications: the MPM – in systems where the broad amplification frequency band is the prevailing parameter, the CMD – in systems where high power, many functions, and high signal quality are of critical importance.

A more detailed analysis of the MPM and CMD parameters would be given in the report.

References:1.Gelvich E.A.,Elektronaya Technika, Ser.Elektronika SVCh,#12,1982; 2.Parker R.K.et al., Microwave Jorn.,March,1992; 3.Ninnis T., Microwave Power Module, L-3 Communication Electron Devices, 2003; 4.Gelvich E.A.,Kotov A.S.,Radiotechnika,#2,2004; 5..Zakurdayev A.D.,Kotov A.S. Radiotechnika,#2,2000; 6..Smith C. R. et al.,Proceedings of the IEEE,v.87,#5,1999; 7..L-3 Communication Electron Devices, Data Book,2003.

TABLE 1 [3] Parameters miniature CMD for application in transmitters.

Frequency band, GHz	X, Ku
Amplification band, %	≤2
Pulse output power, kW	0,3…0,5
Number of operating functions	5
Pulse ratio	3
Carrier frequency switch time, μs	100
Long-term carrier frequency instability, $\Delta f/f$	$\leq 10^{-4}$
Phase noise of the heterodyne channel, dBc/Hz offset from the carrier 5 kHz	-90
Phase noise of the transmitter channel, dBc/Hz off the carrier, kHz	-130 5
Pulse length, μs	0,3…7,5
Intermediate frequency, MHz	<100
MBK cathode operating voltage, kV	2,5
Required voltage stability of power supply source, %	±5
Efficiency, %	25…30
Mass, kg	1,7

Block diagram of a miniature CMD of moderate power (CMD-V)